# Chapter 1

# Introduction

A single layer formed by insoluble amphiphilic molecules at the air-water (A-W) interface is called a Langmuir monolayer. An amphiphilic molecule (Figure 1.1) generally comprises of two parts – hydrophilic (polar) head part and hydrophobic (non-polar) tail part. The hydrophilic part of the amphiphilic molecules can be -COOH, -OH, -CN and -$NH_2$ while the hydrophobic part can be aliphatic chains, aromatic ring systems or the combination of two. The tail can be fluorinated or semifluorinated. The hydrophilic part of the molecule

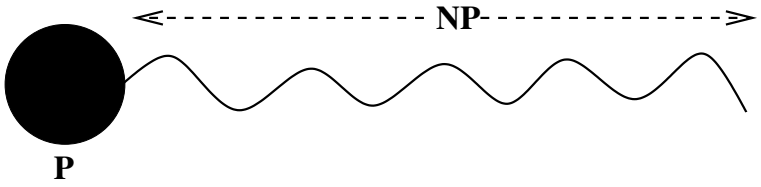


Figure 1.1: A schematic diagram of an amphiphilic molecule. P and NP represent a polar head group and a non-polar tail group, respectively.

can easily form hydrogen bond with water and hence it can stay with water molecules without any appreciable change in the entropy. On the other hand, the hydrophobic part does not form hydrogen bond with water and its inclusion in water may rearrange the water molecules surrounding it. Such an ordering decreases the overall entropy of the system and hence the hydrophobic tail group favours to stay away from the water [1]. In Langmuir monolayer, the hydrophilic part of the amphiphilic molecule gets anchored to the water surface, whereas the hydrophobic part stays away from the surface. This forms a monolayer at the A-W interface. The Langmuir monolayer provides an ideal two-dimensional (2D) system to study the surface thermodynamics where the 2D plane is provided by the smooth

water surface. Langmuir monolayer shows a variety of 2D phases depending on the nature of interaction among the molecules and experimental conditions like temperature, pH and ion contents of the subphase [2]. The stability of the monolayer at the air-water (A-W) interface is determined by the strength of polarity of the head group and the hydrophobic tail group of the molecules. A balance between hydrophilicity and hydrophobicity of the amphiphilic molecule will yield a stable Langmuir monolayer. However, in some special cases, purely hydrophobic materials are also known to form a stable Langmuir monolayer [3]. For instance, semifluorinated alkanes being purely hydrophobic molecules, show a stable Langmuir monolayer at the A-W interface [4, 5]. The formation of such monolayers are attributed to the hydrophobic interaction between the molecules and the increase in overall entropy of the system. There is also a report on the formation of a non-traditional Langmuir monolayer of disubstituted urea lipid molecule where the hydrophilic part stays away from the water surface, whereas the hydrophobic part stays near to the water surface. The stabilization of such monolayer was attributed to the hydrogen bonding network of the urea moiety of the molecule [6].

Langmuir monolayer can be transferred layer by layer on a solid substrate by Langmuir-Blodgett (LB) technique [7]. Hence, Langmuir monolayer serves as a precursor for building LB films. Such films can be used in sensors, molecular electronics, non-linear optical and electrical devices. They find application in the fields of nanolithography, wetting, dewetting, lubrication and friction [7, 8].

There is another kind of monolayer at the A-W interface known as Gibbs monolayer [2, 9]. In Gibbs monolayer, the molecules from the bulk solution adsorb spontaneously at the interface and establish a dynamical equilibrium between the molecules at the interface to the molecules in the solution. Here, the molecules are more hydrophilic and hence soluble in the polar solvent.

The various experimental techniques which we have employed to study the Langmuir monolayer and the LB films are discussed in the next section.

## 1.1 Experimental Techniques

### 1.1.1 Monolayer and multilayer at air-water interface

#### 1.1.1.1 Surface manometry

Surface manometry is a standard technique to study the thermodynamics and the surface phases in a Langmuir monolayer. The presence of a monolayer at the A-W interface reduces the surface tension of water. Such reduction in the surface tension is defined as surface pressure ($\pi$). It is given by

$$\pi = \gamma_o - \gamma \tag{1.1}$$

where $\gamma_o$ is the surface tension of water without monolayer and $\gamma$ is the surface tension with monolayer [2]. In surface manometry, the surface density of the molecules adsorbed at the interface is varied and the surface pressure ($\pi$) is recorded at a constant temperature. This yields a surface pressure - surface density isotherm. The area per molecule ($A_m$) is defined as the inverse of the surface density. The instrument for the measurement of $\pi - A_m$ isotherm is shown in Figure 1.2. It consists of a teflon trough and barriers. The subphase

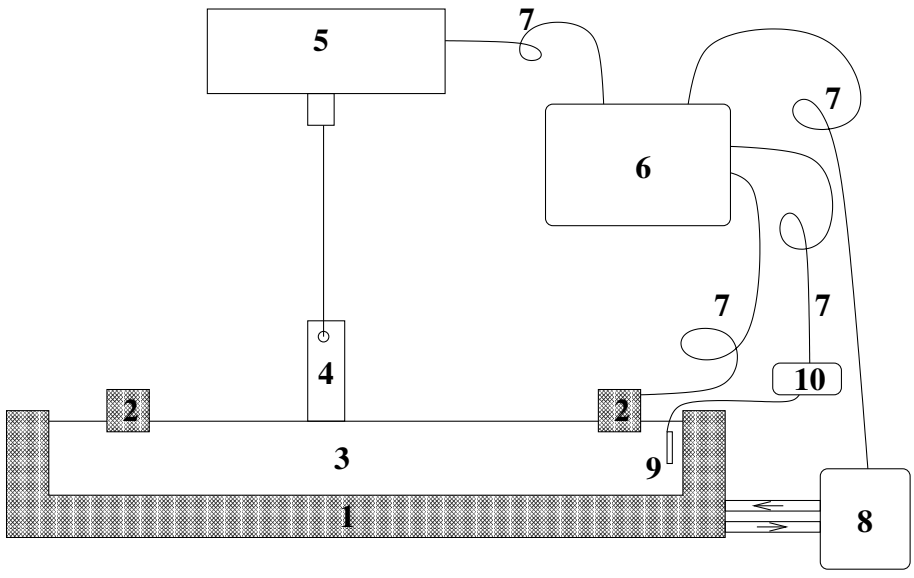


Figure 1.2: A schematic diagram showing the experimental setup for the measurement of surface pressure ($\pi$) - area per molecule ($A_m$) isotherms. The basic parts of the setup are as follows; (1) teflon trough, (2) teflon barriers, (3) subphase (ion-free water), (4) Wilhemy plate (filter paper), (5) surface pressure sensor, (6) computer, (7) connecting wires, (8) thermostat, (9) resistance temperature detector (RTD) and (10) digital multimeter for measuring resistance.

was ultrapure ion-free water having a resistivity greater than 18 MΩ-cm obtained by passing distilled water through filtering and deionizing columns of a Milli-Q Millipore unit. The sample was dissolved in an appropriate solvent to obtain a solution of known concentration. The solution of the samples was spread on the water subphase between the barriers using a precisely calibrated microsyringe (obtained from Hamilton). The solvent was allowed to evaporate for 15 minutes before starting the compression. The surface density of the molecules in the monolayer is varied by changing the area available for the molecules by moving the barriers laterally. The barriers are driven by motors which are controlled by a computer. They are coupled to each other so that it ensures a symmetric compression of the monolayer. The surface pressure was measured using a Wilhemy plate method [2, 10]. We have used filter paper of appropriate size as the Wilhemy plate. The filter paper was suspended from the pressure sensor and was made just to touch the surface of the water. The filter paper was allowed to soak water fully and the reading of the sensor was made zero. The pressure sensor was calibrated such that it gives the value of surface pressure directly. The resolution of the pressure sensor was 0.1 mN/m. The surface pressure and area per molecule at a constant temperature were recorded simultaneously using a computer. This gives the $\pi$-$A_m$ isotherm of the spread molecule. The isotherms at different temperatures are obtained by controlling the temperature of the subphase. This was achieved by circulating water at the required temperature inside the chamber of the trough using a thermostat. The temperature of the subphase was measured by a resistance temperature detector (RTD) and a digital multimeter. A typical $\pi$ - $A_m$ isotherm is shown in Figure 1.3(a). A plateau in the isotherm represents the coexistence of two phases. A kink in the isotherm indicates a phase transition. At a very large area per molecule ($A_m$), the molecules are far apart and do not exert any force on each other. This is a 2D gas phase. On compression, the molecules condense to a low density liquid state ($L_1$). There are no positional and orientational orders in the molecules in this phase. On further compression, the $L_1$ phase transforms to a high density liquid state ($L_2$) accompanied by a two phase ($L_1$+$L_2$) coexisting region. This is known as condensed ($L_2$) phase. In the $L_2$ phase, molecules exhibit a long range orientational order

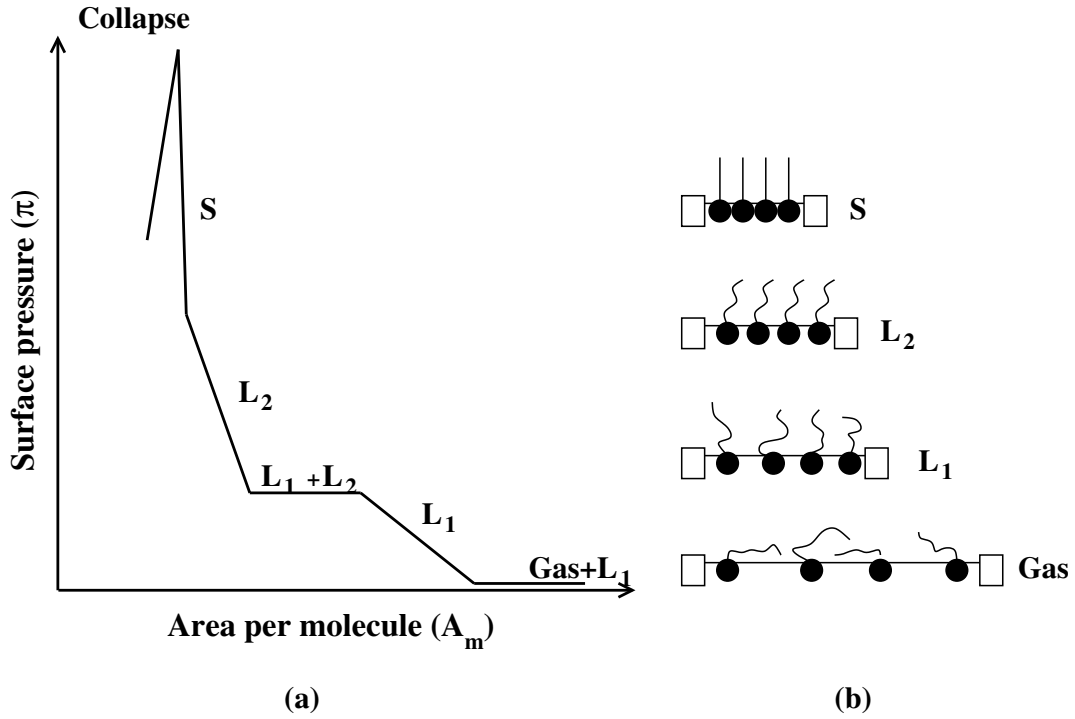


Figure 1.3: (a) shows a typical isotherm indicating the different phases in a Langmuir monolayer. (b) shows the molecular arrangement in the different phases. The symbols $L_1$, $L_2$ and S represent liquid expanded, liquid condensed and solid phases, respectively.

and a quasi-long range positional order. On compression, the $L_2$ phase transforms to a 2D solid (S) phase. On further compression, the monolayer collapses. This is indicated by a sharp decrease in surface pressure.

The area per molecule at which the isotherm indicates very small and finite values of the surface pressure (*e.g.* 0.2 mN/m) is known as lift-off area per molecule ($A_i$). The average area occupied by the molecules in a phase is determined by extrapolating the corresponding region of the isotherm to the zero surface pressure on the $A_m$ axis. The extrapolation of the steep region (*e.g.* S phase in Figure 1.3) of the isotherm to zero surface pressure is called limiting area per molecule ($A_o$). This is the minimum area to which the molecules can be compressed on the water surface without collapsing the monolayer. The orientational state (tilt or untilt) of the molecules in a phase can be estimated qualitatively by comparing the extrapolated area per molecule with that of molecular cross-sectional area in the bulk single crystal.

The isothermal in-plane elastic modulus $E$ is an appropriate quantity for distinguishing

very weak phase transitions. The isothermal in-plane elastic modulus [11] is defined as

$$E = -(A_m) \times (d\pi/d(A_m)) \tag{1.2}$$

The relaxation in the molecular area with time at a given surface pressure can indicate the nature of stability of the monolayer at the interface. A fast reduction in the area with time may indicate an unstable monolayer where the instability can be attributed to dissolution of the molecules to subphase or evaporation. A slow reduction can be attributed to the relaxation of the molecules in the monolayer. The nature and the mechanism of collapse can be studied by monitoring the change in molecular area with time at a constant surface pressure [12]. In some special cases, a kinetic of adsorption of the molecules from the subphase to the monolayer at the interface can be studied. In such cases, the area was found to increase or decrease with time due to complex formation of the molecules in the subphase with the molecules at the interface [13]. It provides a method to study kinetics of the surface chemistry.

The equilibrium spreading pressure [2] is a surface pressure of a monolayer coexisting with its bulk phase at the interface. When a speck of crystallite is placed on the water surface, the molecules from the bulk crystallites elude out and form a monolayer at the interface spontaneously. After a certain period of time, the system reaches an equilibrium state where the rate of elution of molecules from the crystallites is equal to the rate of molecules binding to the crystallites. The variation in surface pressure with time shows an initial increase in surface pressure due to the formation of monolayer. On reaching the equilibrium, the surface pressure value saturates. The saturated value of surface pressure is known as equilibrium surface pressure (ESP). The studies on ESP indicate the spreading capability of the molecules at an interface [2]. The finite value of ESP can suggest the monolayer to be stable against dissolution or evaporation of the molecules. The ESP values of some molecules like stearic acid, octadecanol and dipalmitoyl phosphatidylcholine are 5.2, 34.3 and 1 mN/m, respectively [12].

#### 1.1.1.2 Epifluorescence microscope

In 1981, Tscharner and McConnell [14] have developed the epifluorescence microscopy technique to visualize a monomolecular layer at the A-W interface. The schematic diagram of the experimental setup for the epifluorescence microscopy of the Langmuir monolayer is shown in Figure 1.4. Here, the monolayer (S) was doped with very small quantity

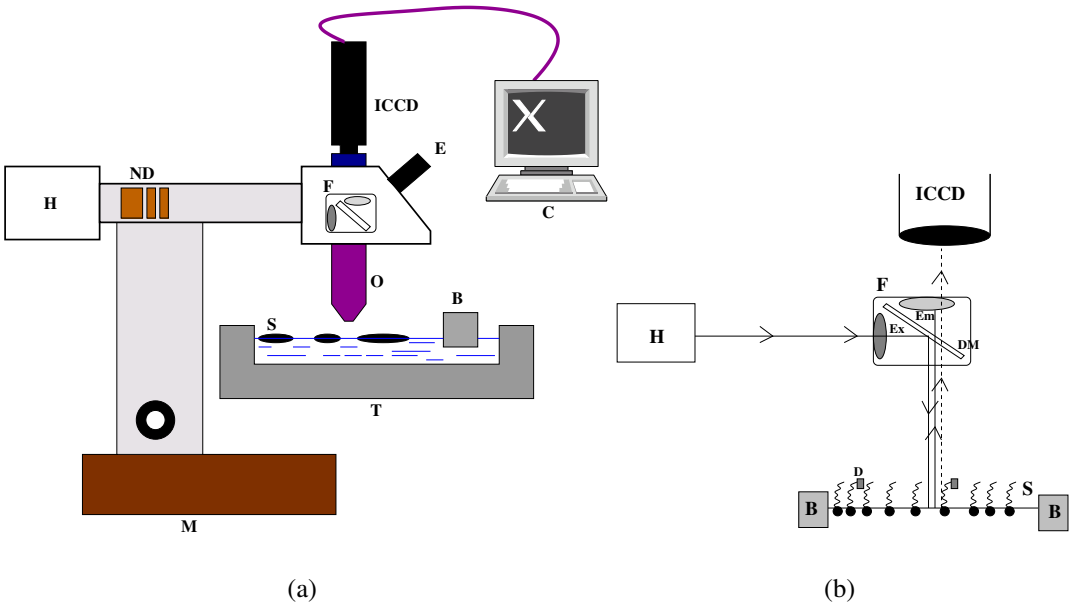


Figure 1.4: Schematic diagram showing the experimental setup for the epifluorescence microscopy. (a) shows a complete microscope setup. (b) shows the working principle of the microscope. The different parts are as follows; high pressure mercury lamp (H), neutral density filter (ND), filter block (F) with emission (Em) and excitation (Ex) filters and a dichroic mirror (DM), objective (O), eye-piece (E), microscope stand (M), intensified charge coupled device (ICCD) camera, computer (C), trough (T), dye doped monolayer (S), dye molecule (D) and barrier (B).

($\leq$ 1 mole%) of an amphiphilic fluorescent dye molecule (D). The dye doped monolayer was observed under an epifluorescence microscope (Leitz Metallux 3). The microscope was equipped with a high pressure mercury lamp (H) and a filter block (F). The filter block consists of an emission filter (Em), an excitation filter (Ex) and a dichroic mirror (DM). The excitation filter allows the light of appropriate wavelength to excite the dye molecules in the monolayer. The reflected light from the interface and emitted light from the dye doped monolayer was allowed to pass through the emission filter (Em) which allows only the emitted light. The emitted light was collected using an intensified CCD camera (ICCD)

and the images were digitized using a frame grabber (National Instruments, PCI-1411). The intensity of the emitted light depends on the miscibility of the dye molecules in a particular phase of the monolayer. The gas phase appears dark due to the quenching of the dye molecules. The liquid expanded phase appears bright in the epifluorescence images. On the other hand, the solid phase appears dark. This is due to the expulsion of dye molecules from the highly dense solid domains. In all the epifluorescence microscopy experiments, we have utilized 4-(hexadecylamino)-7-nitrobenz-2 oxa-1,3 diazole (obtained from Molecular Probes) as an amphiphilic fluorescent molecule.

#### 1.1.1.3 Brewster angle microscope

The epifluorescence microscopy on the Langmuir monolayer has certain disadvantages. For instance, the fluorescent dye acts as an impurity and may alter the phase diagram. There are difficulties in determining the surface phases at the higher surface pressures where the dye molecules are practically insoluble in the domains. Also the photo-bleaching can result in the decomposition of the dye molecules. To overcome such disadvantages, a microscope which works on the principle of Brewster angle, was developed. The microscope is known as the Brewster angle microscope [15,16]. The angle of incidence at which an unpolarized light acquires a linearly polarized state after reflection from the plane of an interface is known as Brewster angle of the reflecting material. The state of polarization of the reflected light at the Brewster angle ($\theta_B$) is perpendicular (s-polarized) to the plane of incidence. At Brewster angle of incidence

$$tan(\theta_B) = n_2/n_1 \tag{1.3}$$

where $n_2$ is the refractive index of the reflecting material and $n_1$ is the refractive index of the medium through which the light is incident. We have utilized a commercial setup, MiniBAM Plus from Nanofilm Technologie for BAM imaging. In the microscope, a polarized light source from a 30 mW laser of wavelength 660 nm falls on the water surface at the Brewster angle (~53°). The reflected light is allowed to pass through a polarizer which allows only the p-component of the reflected light to enter a CCD camera, as shown in Figure 1.5. Since the

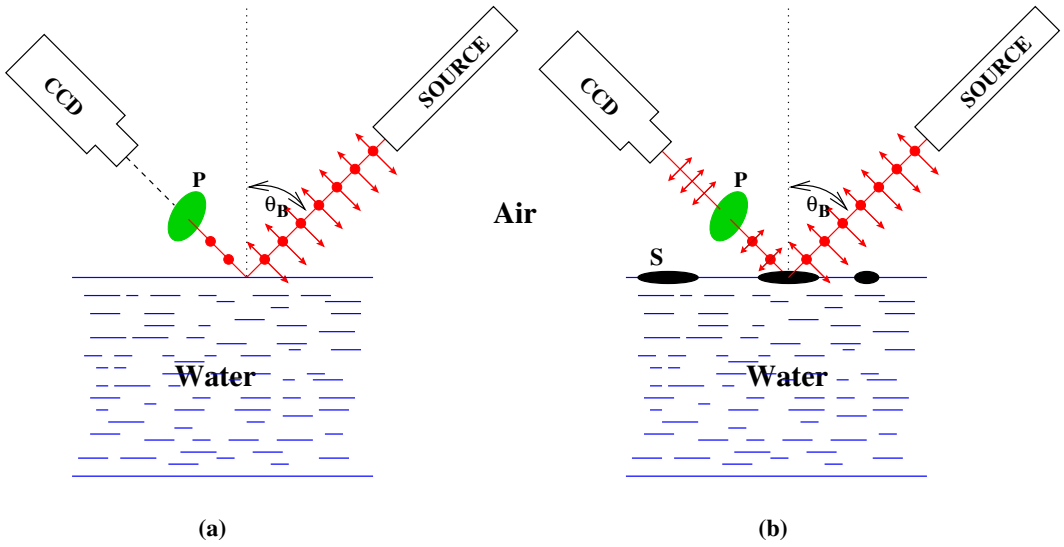


Figure 1.5: Schematic diagrams showing the working principle of a Brewster angle microscope. $\theta_B$ is the Brewster angle of water with respect to air. The different parts are as follows; polarizer (P), charge coupled device (CCD) camera and monolayer at the air-water interface (S). (a) and (b) are the BAM setups without and with monolayer at the A-W interface, respectively.

angle was set for the Brewster angle of water, the reflected intensity in the CCD camera was minimum for pure water. Therefore, any domain of the monolayer changes the refractive index at the interface and hence the Brewster angle for A-W interface gets altered. This in turn reflects some light which was collected by the CCD to form the images of the monolayer domains. The intensity of the reflected light depends on the thickness of the film and the surface density of the molecules. The optical anisotropy in the BAM images arises due to a difference in tilt-azimuth variation of the molecules in the monolayer and the anisotropy in the unit cell [17].

### 1.1.2 Monolayer and multilayer at air-solid interface

Langmuir-Blodgett (LB) technique can be employed to form monolayer or multilayer films at the solid-air interface. In this technique, the monolayer in a particular phase at the A-W interface can be transferred layer by layer onto a solid substrate by vertically moving the substrate in and out of the subphase. During deposition, the surface pressure is fixed at some target value known as target surface pressure ($\pi_t$). The experimental setup for LB deposition is shown in Figure 1.6. The setup is similar to that of the Langmuir trough except

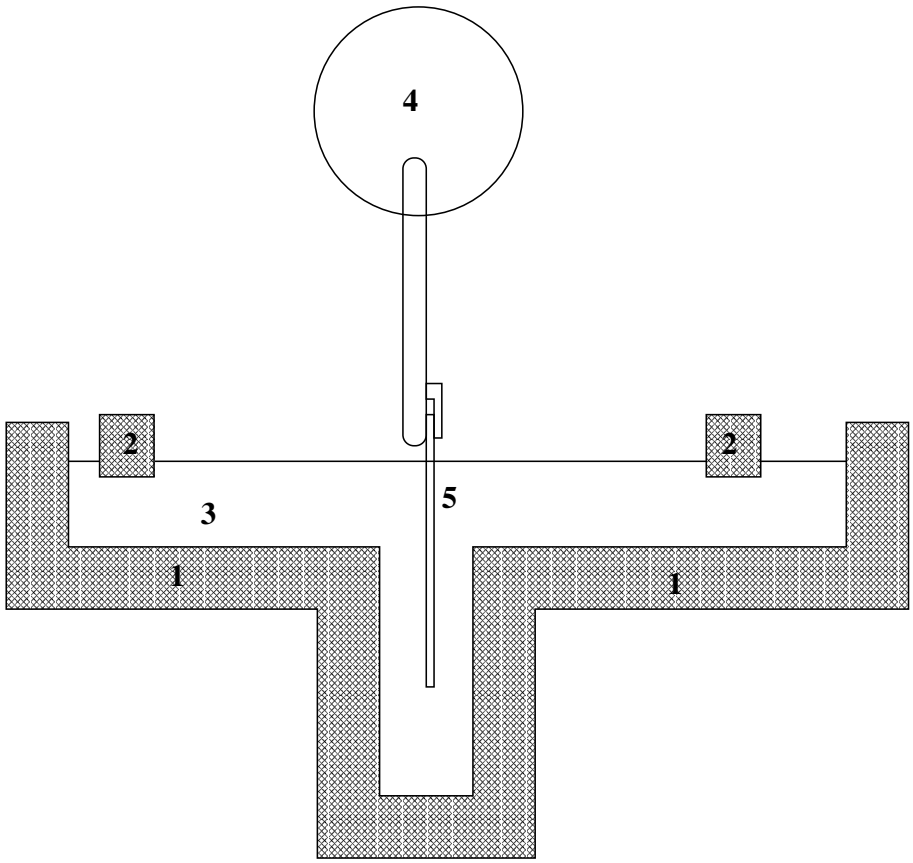


Figure 1.6: A schematic diagram showing the experimental setup for forming Langmuir-Blodgett films. The parts are as follows; (1) teflon trough with a well in the center, (2) barriers, (3) subphase, (4) dipper and (5) substrate.

it possesses a well in the teflon trough and a dipper. For the LB film transfer, the trough has a motorized dipper which holds the substrate and it can be moved up and down very precisely. Such a motion makes the substrate to dip in and out of the subphase with a monolayer at the interface. During deposition, the surface pressure is fixed at $\pi_t$ by a feedback mechanism. The barriers compress the monolayer until the $\pi_t$ is attained. Any increase or decrease in surface pressure is fed back to the computer which in turn moves the barrier to maintain the required target surface pressure. The mechanism of building multilayer by LB technique is shown in Figure 1.7(a). The efficiency of transfer of the monolayer on the solid substrate is estimated by measuring the transfer ratio ($\tau$). The transfer ratio ($\tau$) is defined as [7]

$$\tau = \frac{\text{area of monolayer transferred from the A} - \text{W interface}}{\text{area of the substrate to be deposited}} \tag{1.4}$$

The value of $\tau$ equal to one indicates defectless LB film. There are different types of LB deposition. If the monolayer transfers during both the upstroke and downstroke of the dipper,

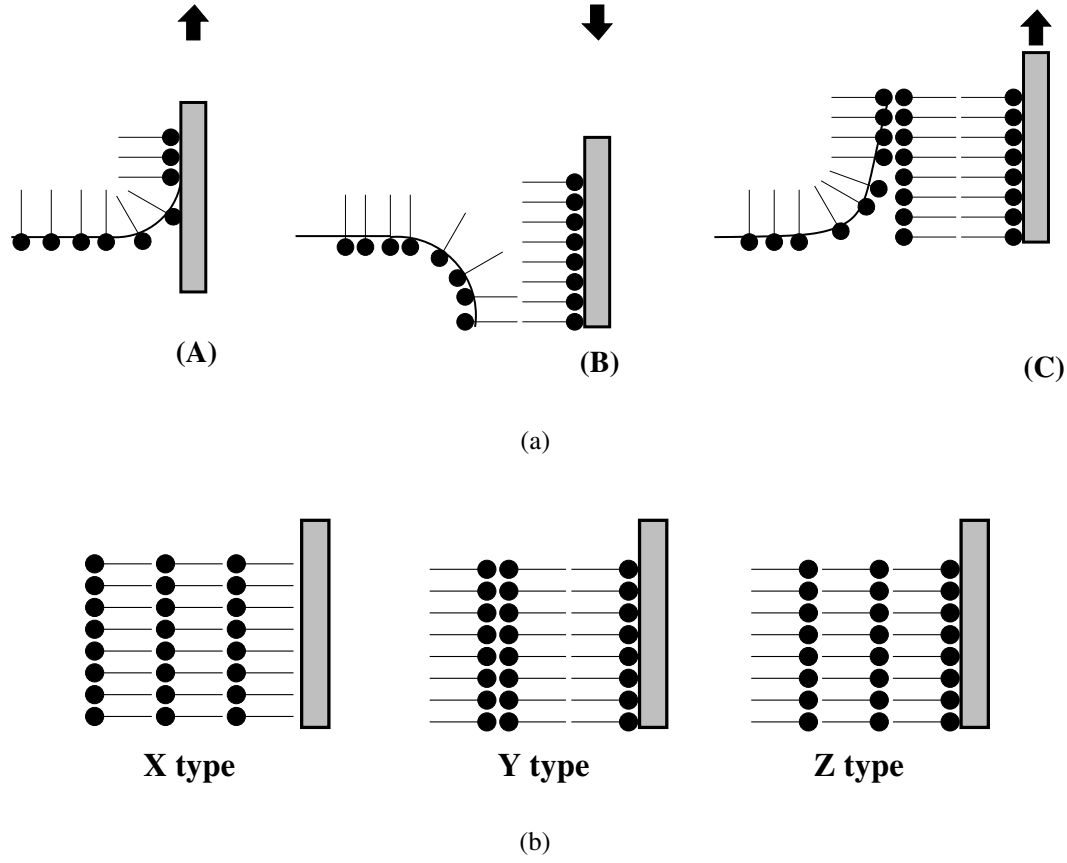


Figure 1.7: (a) depicts the mechanism of formation of multilayer by the Langmuir-Blodgett technique. (A) first upstroke, (B) first downstroke and (C) second upstroke. (b) shows the structure of different types of multilayer obtained by LB technique, namely X-, Y- and Z-type.

such deposition is known as Y-type of LB deposition. On the other hand, if the deposition takes place only with either downstrokes or upstrokes, they are termed as X or Z-type of LB deposition, respectively (Figure 1.7(b)). Sometimes a combination of these depositions are also observed [7]. The negative values of $\tau$ indicate desorption. The LB depositions are dependent on the nature of interaction between the substrate and the molecules, dipper speed, target surface pressure, ion contents of the subphase and temperature. We have employed a Langmuir-Blodgett trough procured commercially from NIMA (model 611M) for both surface manometry studies and LB film deposition.

The monolayer at the A-W interface can be transferred onto substrates by two other

different techniques. These are called horizontal transfer method and Schaefer's method. In the horizontal transfer method, the substrate is immersed horizontally in the subphase and then the monolayer is formed at the A-W interface. Then the aqueous subphase is siphoned out very slowly from the other side of the barriers. The monolayer gets adsorbed onto the substrate as the water drains out. In the Schaefer's method, a hydrophobic substrate is allowed to touch the monolayer on the water surface. The hydrophobic part of the molecules get adsorbed to the substrate. To facilitate the drainage of water, the substrates in either case can be tilted by a small angle prior to the adsorption.

#### 1.1.2.1 Scanning probe microscopes

The discovery of scanning probe microscopes by Binning and coworkers has revolutionized the field of surface science. Its versatile range of applications have made it an indispensable tool in the fields of surface science and other branches of soft condensed matter. It is useful in the study of the surface topography, electronic properties of the film, film growth, adhesion, friction, lubrication, dielectric and magnetic properties. It has also been used in a molecular or atomic manipulation. Among the various scanning probe microscopes, scanning tunneling [18, 19] and atomic force microscopes [20] are widely used to study LB films.

The schematic diagram of the STM is shown in Figure 1.8. In scanning tunneling microscope, a very sharp metallic tip (T) is brought very close to a conducting substrate (S). The substrate may be coated with a film (F). When a low bias voltage ($\sim$1 V) is applied between the tip and the substrate, a tunneling current flows between them. STM works in two modes − constant current (CC) mode and constant height (CH) mode. While scanning the surface in CC mode, the tunneling current between the tip and the sample is kept constant. In this mode, the height of the tip is adjusted automatically using a feedback circuit to achieve the constant tunneling current. The variation in tip height (z) as a function of lateral coordinates (x,y) gives the topographic information of the sample. In CH mode, the height of the tip is kept constant and the tunneling current is recorded as a function of (x,y). The

CH mode provides the electronic information of the sample.

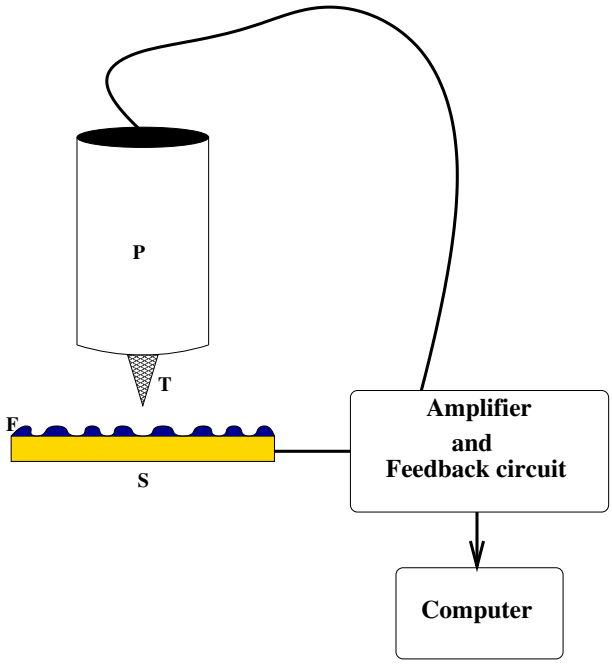


Figure 1.8: Schematic diagram of a scanning tunneling microscope (STM). The parts are as follows; conducting substrate (S), film (F), metallic tip (T) and piezo tube (P).

Atomic force microscope (AFM) gives the topographic images by sensing the atomic forces between a sharp tip and the sample. A schematic diagram of an AFM is shown in Figure 1.9. Here, the tip is mounted on a cantilever. The head of the tip is coated with a reflecting material like gold and it is illuminated by a laser light. The reflected light is collected on a quadrant photodiode. Any deflection in the tip due to its interaction with the sample is monitored by measuring a distribution of light intensity in the photodiode. There are numerous modes of operation of AFM. We have utilized tapping mode and contact mode of AFM. In contact mode, the tip is brought into direct contact with sample and the surface is scanned. It is also known as constant force mode. Here, the force between the tip and the sample is kept constant and by monitoring the bending of the cantilever as a function of (x,y), a topographic image can be obtained. In tapping mode, the tip is allowed to oscillate nearly to its resonant frequency on the sample at a given amplitude and frequency. Due to interaction between the tip and the sample, the amplitude and phase of oscillation of the tip change. The change in amplitude can be used to obtain a topographic map of the sample.

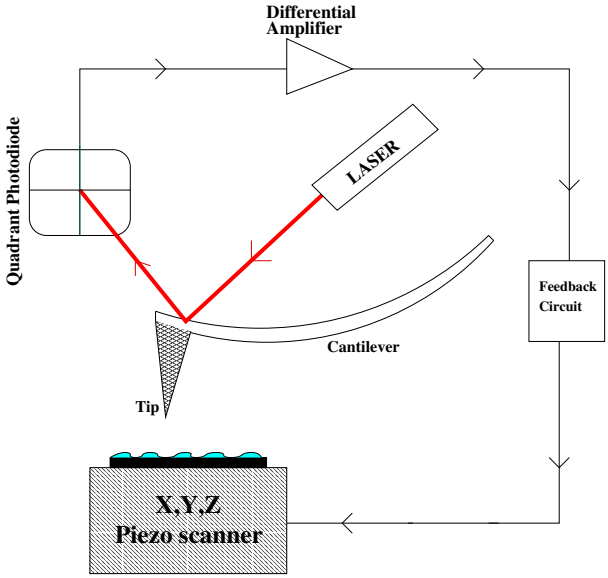


Figure 1.9: Schematic diagram of an atomic force microscope (AFM).

The phase change gives an insight about the chemical nature of the sample.

#### 1.1.2.2 Grazing angle reflection absorption infrared spectroscopy

The interaction between the infrared radiation and the transition dipole moment associated with the molecules in a film can be enhanced either by allowing the IR beam to interact with the film multiple times or if it is incident on the film at a grazing angle. The former principle is utilized in attenuated total reflection, whereas the latter is known as grazing angle reflection absorption infrared spectroscopy (RAIRS). The tilt of the molecules in the ultrathin films (like LB films or self-assembled monolayers) can be determined using this technique. Figure 1.10 shows a schematic diagram of the setup. The absorbance ($I$) of IR band due to the vibration of the IR active species having a transition dipole moment $M$ is given by

$$I = (ME)^2 cos^2\theta \tag{1.5}$$

where $E$ is the magnitude of the incident electric field and $\theta$ is the angle between the $E$ and $M$. The value of $\theta$ and hence the molecular orientation in an ultrathin film can be determined employing the Equation 1.5. In Appendix B, we discuss in detail the design, fabrication, and calibration of a variable temperature grazing angle reflection absorption infrared spectroscopy developed by us in the laboratory.

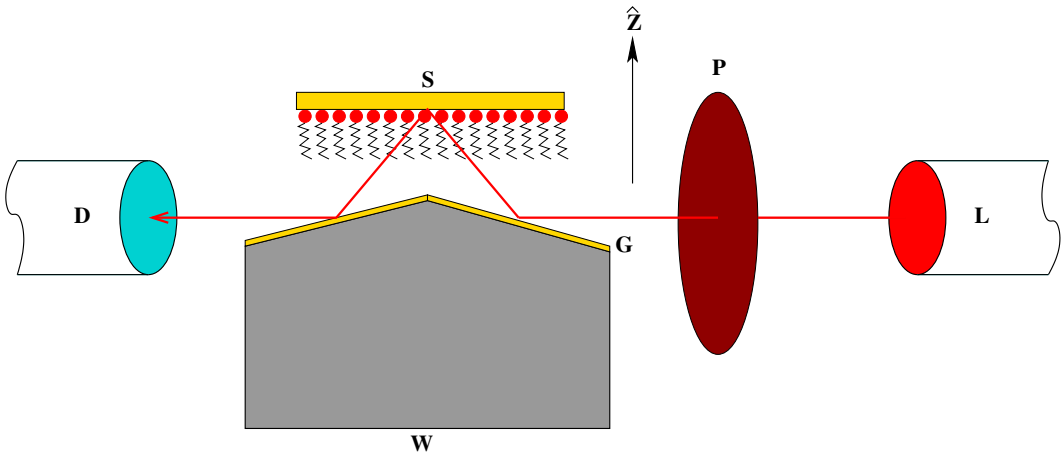


Figure 1.10: A schematic diagram showing the reflection absorption infrared spectroscopy (RAIRS) setup. The different parts are as follows: infrared source (L), IR polarizer (P), substrate with a monolayer (S), copper wedge (W), gold reflector (G) and detector (D).

## 1.2 Two-dimensional phases in Langmuir monolayer

Langmuir monolayer can exhibit a number of phases depending on the surface density. Conventionally, a kink in the isotherm indicates a phase transition. The weak transition can also be detected by calculating the in-plane elastic modulus (or 2D compressibility). A detailed information on the phases of Langmuir monolayer is reviewed in the reference [21]. Some of the phases detected using an $\pi$ - $A_m$ isotherm and microscope observations are described below.

*Gas phase* : At a very large area per molecule ($A_m$), the molecules are separated sufficiently enough to have no interaction among each other. The gas (G) phase is identified experimentally by the zero surface pressure region of the isotherm at large $A_m$. In epifluorescence microscopy, it reveals a dark region due to quenching of the dye molecules. The BAM imaging reveals dark region for the gas phase due to very low surface density of the molecules. In the case of an ideal 2D gas, the equation of state can be written as

$$\pi A_m = k_B T \tag{1.6}$$

where $k_B$ is the Boltzmann constant and $T$ is absolute temperature. This is the case for a non interacting gas particles. However the molecules in the Langmuir monolayer can have coulombic, dipolar or van der Waals interactions. In a simple case, assuming a van der Waals

interaction among the molecules, we can write the equation of state as

$$(\pi + \frac{a^2}{A_m})(A_m - b) = k_B T \tag{1.7}$$

where $a$ and $b$ are constants.

*Liquid expanded phase* : Liquid expanded or $L_1$ phase is a low density liquid phase where there is no positional order in the head and orientational order in the tail groups. The phase is identified experimentally by the onset of a slow or gradual rise in surface pressure in the isotherm. Epifluorescence microscopy shows an uniform texture for the $L_1$ phase. The BAM image shows an uniform texture for this phase.

*Liquid condensed phase* : Liquid condensed phase or $L_2$ phase is a high density liquid phase with a long range orientational order in the tail group. There is a quasi-long range positional order in the head group. Depending upon positional and orientational orders, there are various sub-classifications of the liquid condensed phase. These classifications were made using the results from high resolution BAM [17, 22], polarized fluorescence microscopy [23] and grazing angle X-ray diffractions [21, 24, 25]. However, due to the limitation of our experimental setup, we were not able to distinguish the various sub-phases of the liquid condensed monolayer. In the $\pi - A_m$ isotherm, the condensed phase is identified as a steep rise in the surface pressure. The phase is less compressible and it shows higher values of in-plane elastic modulus as compared to the liquid expanded phase. In epifluorescence image, it shows an uniform texture. However, it is less intense as compared to the expanded phase. The condensed phase can be tilted or untilted. We denote $L_2$ for the untilted condensed phase.

*Solid phase* : This is a highly dense, nearly incompressible 2D solid (S) phase. In this phase, the molecules usually orient normal to the interface. The in-plane elastic modulus of the phase is very high (~1000 mN/m for stearic acid monolayer). The epifluorescence

images show dark domains of the solid phase due to the expulsion of the dye molecules. The BAM images show an uniform bright texture.

*Collapsed state* : The collapsed state is generally indicated either by a sharp decrease in the surface pressure or a plateau in the isotherm. In the collapsed state, the molecules try to go to the third dimension. A plateau in the collapse state indicates the formation of multilayer, whereas a sharp decrease indicates a random crystallization into the 3D crystals. The nature of collapse varies from molecules to molecules. It also depends on the experimental conditions. The monolayer may fold or bend in the collapsed state [26].

A Langmuir monolayer of aliphatic chain derivatives is known to exhibit 17 different surface phases [21, 27]. This is shown in Figure 1.11.

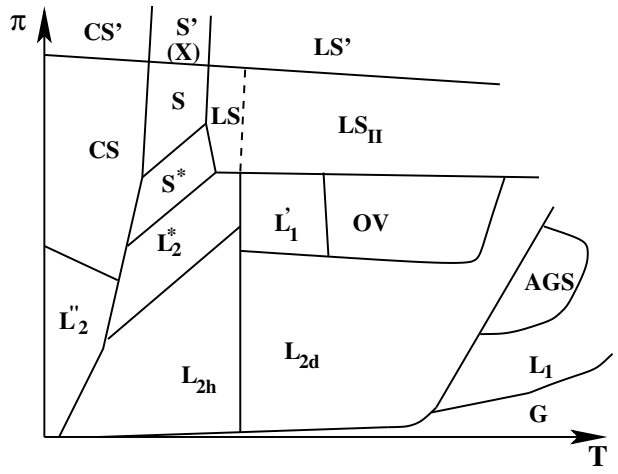


Figure 1.11: Phase diagram showing the monolayer phases of aliphatic chain derivatives [27]. T and $\pi$ represent temperature and surface pressure, respectively. The symbols G, $L_1$ and AGS represent the gas, liquid expanded and fluid lamellar phases, respectively. The phases denoted by $L_{2d}$, $L_{2h}$, $L_2^{''}$, $L_2^*$ and OV are the various sub-classifications of liquid condensed phase. The symbols CS, CS$^{'}$, S, S$^*$, S$^{'}$, LS, $LS_{II}$, and LS$^{'}$ represent the various solid phases.

The molecules in the Langmuir monolayer may tilt due to an anisotropy in the size of head-tail group [28]. Such tilting may results in the various patterns seen under the microscope.

## 1.3 Mixed monolayers

Mixed monolayers are of considerable interest in many systems like biological membranes. They have been extensively studied. It provides useful information regarding the interaction and orientation of the component molecules. For example, a monolayer study on lung surfactant (complex mixture of many components) provides an useful information regarding a collapse mechanism of the lung surfactant during exhalation process [29]

The miscibility of the component molecules is of considerable interest. The collapse pressure ($\pi_c$) of mixed monolayer can indicate qualitatively a miscible or a non-miscible nature of the component molecules. If the $\pi_c$ lies in the range of the collapse pressures of individual components, the mixed monolayer is said to be miscible. On the other hand, if the mixed monolayer shows two collapses corresponding to the individual components, it is said to be immiscible. In the mixed monolayer, the area per molecule at a given surface pressure may deviate from the ideal case. Such a deviation in the $A_m$ is called as excess area per molecule ($A_{ex}$). A positive or negative value of $A_{ex}$ suggests a repulsive or an attractive interaction between the component molecules.

## 1.4 Molecules forming Langmuir monolayer and Langmuir-Blodgett films

There is a class of molecules which shows some intermediate phases (mesophases) between crystalline and isotropic liquid phases. These molecules are known as mesogenic molecules or mesogens. Mesogens are of two types - thermotropic and lyotropic. Thermotropic molecules show mesophases on varying the temperature, whereas the lyotropic molecules show mesophases in solutions necessarily on varying concentration. The lyotropic mesophases also depend on temperature, and other physical parameters. Some of the thermotropic mesogens, possessing a polar and a non-polar part, also form Langmuir monolayer. Such mesogens are called amphotropic molecules. Some of the most commonly studied amphotropic molecules are rod-shaped [30, 31] and disk-shaped [32].

Clusters of metallic atoms can be functionalized chemically with organic ligands to furnish it with an amphiphilic nature. We call such molecules as organometallic, that is the organic ligands to the metallic clusters. Such functionalized molecules when spread on the water surface yield a stable Langmuir monolayer and show a variety of surface phases.

Amphiphilic molecules are ubiquitous in biological systems. The lipids (e.g. fatty acids, phopholipids, cholesterol and cholesteryl esters) are the basic constituents of the cell membrane and are amphiphilic in nature. There are extensive studies on the Langmuir monolayer and LB films of lipid molecules. Some polymers (including biopolymers) are also known to assemble on water surface to form a Langmuir monolayer [33–35].

In this thesis, we have studied the monolayer of a sterol possessing amphotropic molecule (cholesteric acid) with a size anisotropy in the head and tail groups. The effect of presence of molecules of different structures on the phases of cholesteric acid (ChA) was studied and the stability as well as miscibility of such mixed monolayers were addressed. The role of hydrophobic sterol moiety of cholesterol in stabilizing the monolayer of a non-amphiphilic sterol molecule (thiocholesterol) was studied. The LB films of cholesterol on a chemically treated hydrophobic glass substrate was studied using AFM. Here, AFM study reveals very interesting patterns like doughnuts and so on. The STM study on the LB films of cholesterol on smooth graphite substrate reveals a highly ordered structure with a planar orientation of the molecules. Such an observation is confirmed by computer simulations. Our study on the monolayer of an amphiphilic discotic liquid crystal shows a stable phase of the coexistence of both the face-on and edge-on conformations of the molecules at the A-W interface. The monolayer of an amphiphilic functionalized gold particle at various temperature was studied. We have probed the stability of the Langmuir monolayer of the octadecanethiol molecule on the A-W interface and studied the LB films formed on atomically smooth silicon substrate.

# Bibliography


[1] J. N. Israelachvili, *Intermolecular and Surface Forces : With Applications to Colloidal and Biological Systems* (Academic Press, London, 1992).

[2] G. L. Gaines, Jr., *Insoluble Monolayers at Liquid-Gas Interfaces* (Wiley-Interscience, New York, 1966).

[3] Y. Tabe, T. Yamamoto, I. Nishiyama, K. M. Aoki, M. Yoneya, and H. Yokoyama, J. Phys. Chem. B **106**, 12089 (2002).

[4] G. L. Gaines Jr., Langmuir **7**, 3054 (1991).

[5] A. El Abed, M-C. Fauré, E. Pouzet, and O. Abillon, Phys. Rev. E **65**, 051603 (2002).

[6] Q. Huo, S. Russev, T. Hasegawa, J. Nishijo, J. Umemura, G Puccetti, K. C. Russell, and R. M. Leblanc, J. Am. Chem. Soc. **122**, 7890 (2000).

[7] G. Roberts, *Langmuir-Blodgett Films* (Plenum, New York, 1990).

[8] A. Ulman, *An Introduction to Ultrathin Organic Films From Langmuir-Blodgett to Self-Assembly* (Academy Press Inc., San Diego, 1991).

[9] V. Melzer, D. Vollhardt, G. Brezesinski, and H. Möhwald, J. Phys. Chem. B **102**, 591 1998.

[10] A. W. Adamson, *Physical Chemistry of Surfaces* (Wiley-Interscience, New York, 1990).

[11] R. Lipowsky and E. Sackmann, *Handbook of Biological Physics* (Elsevier Science,Amsterdam, 1995) Chapter 4.

[12] R. D. Smith and J. C. Berg, J. Colloid Interface Sci., **74**, 273 (1980).

[13] V. Ramakrishnan, M. D Costa, K. N. Ganesh, and M. Sastry, Langmuir **18**, 6307 (2002).

[14] V. von Tscharner and H. M. McConnell, Biophys. J. **36**, 409 (1981).

[15] D. Hönig and D. Möbius, J. Phys. Chem. **95**, 4590 (1991).

[16] S. Hénon and J. Meunier, Rev. Sci. Instrum. **62**, 936 (1991).

[17] S. Rivière, S. Hénon, J. Meunier, D. K. Schwartz, M.-W. Tsao, and C. M. Knobler, J. Chem. Phys. **101**, 10045 (1994).

[18] G. Binning and H. Rohrer, Helv. Phys. Acta **55**, 726 (1982).

[19] G. Binning, H. Rohrer, Ch. Geber, and E. Weibel, Phys. Rev. Lett. **49**, 57 (1982).

[20] G. Binning, C. F. Quate, and Ch. Gerber, Phys. Rev. Lett. **56**, 930 (1986).

[21] V. M. Kaganer, H. Möhwald, and P. Dutta, Rev. Mod. Phys. **71**, 779 (1999).

[22] G. A. Overbeck and D. Möbius, J. Phys. Chem. **97**, 7999 (1993).

[23] D.K. Schwartz and C. M. Knobler, J. Phys. Chem. **97**, 8849 (1993).

[24] V. M. Kaganer, I. R. Peterson, R. M. Kenn, M. C. Shih, M. Durbin, and P. Dutta, J. Chem. Phys. **102**, 9412 (1995).

[25] J. Als-Nielsen, D. Jacquemain, K. Kjaer, F. Leveiller, M. Lahav, and L. Leiserowitz, Phys. Rep. **246**, 251 (1994).

[26] H. E. Ries, Nature (London) **281**, 287 (1979).

[27] I. R. Peterson and R. M. Kenn, Langmuir **10**, 4645 (1994).

[28] S. A. Safran, Mark O. Robbins, and S. Garoff, Phys. Rev. A **33**, 2186 (1986).

[29] W. R. Schief, M. Antia, B. M. Disher, S. B. Hall, and V. Vogel, Biophys. J. **84**, 3792 (2003).

[30] M. F. Danier, O. C. Lettington, S. M. Small, Thin Solid Films **99**, 61 (1983).

[31] Y. Tabe, N. Shen, E. Mazur, and H. Yokoyama, Phys. Rev. Lett. **82**, 759 (1999).

[32] F. Rondelez, D. Koppel, and B. K. Sadashiva, J. Phys. (Paris) **43**, 1361 (1982).

[33] K. S. Birdi, *Lipid and Biopolymer Monolayers at Liquid Interfaces* (Plenum, New York, 1989).

[34] F. Monroy, H. M. Hilles, F. Ortega, and R. G. Rubio, Phys. Rev. Lett. **91**, 268302 (2003).

[35] J. Kim and T. M. Swager, Nature (London) **411**, 1030 (2001).